Abnormal variation of magnetic properties with Ce content in $(PrNdCe)_2Fe_{14}B$ sintered magnets prepared by dual alloy method*

Xue-Feng Zhang(张雪峰)[1,2], Jian-Ting Lan(兰剑亭)[1,2], Zhu-Bai Li(李柱柏)[1,†], Yan-Li Liu(刘艳丽)[1,2], Le-Le Zhang(张乐乐)[1,2], Yong-Feng Li(李永峰)[1,2], and Qian Zhao(赵倩)[1,2]

[1] *Key Laboratory of Integrated Exploitation of Bayan Obo Multi-Metal Resources, Inner Mongolia University of Science and Technology, Baotou* 014010, *China*

[2] *School of Mathematics, Physics and Biological Engineering, Inner Mongolia University of Science and Technology, Baotou* 014010, *China*

(Received 19 December 2015; revised manuscript received 28 January 2016; published online 31 March 2016)

Resource-saving $(PrNdCe)_2Fe_{14}B$ sintered magnets with nominal composition $(PrNd)_{15-x}Ce_xFe_{77}B_8$ ($x = 0$–10) were prepared using a dual alloy method by mixing $(PrNd)_5Ce_{10}Fe_{77}B_8$ with $(PrNd)_{15}Fe_{77}B_8$ powders. For Ce atomic percent of 1% and 2%, coercivity decreases dramatically. With further increase of Ce atomic percent, the coercivity increases, peaks at 6.38 kOe in $(PrNd)_{11}Ce_4Fe_{77}B_8$, and then declines gradually. The abnormal dependence of coercivity is likely related to the inhomogeneity of rare earth chemical composition in the intergranular phase, where PrNd concentration is strongly dependent on the additive amount of $(PrNd)_5Ce_{10}Fe_{77}B_8$ powders. In addition, for Ce atomic percent of 8%, 7%, and 6% the coercivity is higher than that of magnets prepared by the conventional method, which shows the advantage of the dual alloy method in preparing high abundant rare earth magnets.

Keywords: permanent magnets, Ce element, dual alloy method, coercivity

PACS: 75.50.Vv, 75.50.Ww **DOI:** 10.1088/1674-1056/25/5/057502

1. Introduction

$(PrNd)_2Fe_{14}B$ permanent magnets are a high energy product and are widely used in numerous devices, promoting the technology development in the areas of computers, motors, miniature speakers, and wind turbines, etc.[1–3] However, their mass production and wide application give rise to the unbalanced use of rare earth and the backlog of Ce.[4–11] Ce ion is in a strongly mixed-valent α-like state rather than the trivalent γ state, so it is nonmagnetic and the magnetocrystalline anisotropy is low in $Ce_2Fe_{14}B$.[12,13] Furthermore, the phase diagram and phase constitution of Ce–Fe–B are different from those of Nd–Fe–B,[14,15] and the minor phases possibly lead to a large variation of magnetic properties. It is a big challenge to obtain relatively high magnetic properties in the resource-saving and low cost $Ce_2Fe_{14}B$ magnets using the conventional sintered method.[16–19] The rare earth substitution could optimize the phase constitution and thus enhance the coercivity in $(PrNdCe)_2Fe_{14}B$ magnets,[20–22] and the dual alloy method is a feasible way to improve the magnetic properties by mixing $(NdCe)_2Fe_{14}B$ with $Nd_2Fe_{14}B$ powders.[23] For reducing the cost of this type of magnet, the amount of Ce should be further increased in the resource-saving permanent magnets, therefore, it is necessary to probe how the Ce element affects the magnetic properties in $(PrNdCe)_2Fe_{14}B$ magnets. In this paper, we investigate the magnetic properties of $(PrNdCe)_2Fe_{14}B$ sintered magnets prepared by mixing Ce-rich powders of $(PrNd)_5Ce_{10}Fe_{77}B_8$ (the atomic ratio of Pr/Nd is 0.8) with $(PrNd)_{15}Fe_{77}B_8$ powders. It is found that the coercivity is abnormally dependent on the Ce content, and that in high Ce content magnets prepared by the dual alloy method the coercivity is higher than that of conventional sintered magnets. It is expected that these investigations could serve as a reference for optimizing the composition designing in preparing high abundant rare earth magnets.

2. Experiment

Two kinds of ingots with nominal compositions $(PrNd)_5Ce_{10}Fe_{77}B_8$ and $(PrNd)_{15}Fe_{77}B_8$ were prepared, respectively, by induction melting of PrNd, Ce, Fe and FeB under the protection of high-purity argon. The 1 wt% excessive of rare earth elements was used to compensate the weight loss in the induction melting process. The ingots were broken to small pieces and then crushed to powders in a grinder. $(PrNd)_5Ce_{10}Fe_{77}B_8$ and $(PrNd)_{15}Fe_{77}B_8$ powders were mixed in molar ratios of 0, 1/10, 1/5, 3/10, 2/5, 1/2, 3/5, 7/10, 4/5, 9/10, and 1, respectively, corresponding to the nominal compositions of $(PrNd)_{15}Fe_{77}B_8$, $(PrNd)_{14}Ce_1Fe_{77}B_8$, $(PrNd)_{13}Ce_2Fe_{77}B_8$, $(PrNd)_{12}Ce_3Fe_{77}B_8$, $(PrNd)_{11}Ce_4Fe_{77}B_8$, $(PrNd)_{10}Ce_5Fe_{77}B_8$, $(PrNd)_9Ce_6Fe_{77}B_8$, $(PrNd)_8Ce_7Fe_{77}B_8$, $(PrNd)_7Ce_8Fe_{77}B_8$, $(PrNd)_6Ce_9Fe_{77}B_8$, and $(PrNd)_5Ce_{10}Fe_{77}B_8$. Ball milling was performed in petroleum ether for 45 min and the particle

*Project supported by the National Natural Science Foundation of China (Grant Nos. 51461033, 51571126, 51541105, and 11547032), the Natural Science Foundation of Inner Mongolia, China (Grant No. 2013MS0110), and the Inner Mongolia University of Science and Technology Innovation Fund, China.

†Corresponding author. E-mail: lzbgj@163.com

© 2016 Chinese Physical Society and IOP Publishing Ltd

size were decreased to 3–5 μm. The fine mixed powders were compacted to green pellets after alignment under a 2 T pulsed magnetic field and then cold isostatic pressed at 300 MPa. The vacuum sintering was carried out at 1040–1080 °C for 2 h, and then the as-sintered magnets were annealed at 900 °C and 600 °C for 2–4 h, respectively. With the increase of Ce content, the sintering temperature was decreased correspondingly for optimizing the coercivity. Magnetic properties were measured using a NIM-200C hysteresis graph. The phase constitution, microstructure and chemical composition of the intergranular phase were observed by x-ray diffraction (XRD) spectrum, backscattered electron (BSE) of a scanning electron microscope (SEM), and an energy dispersive spectrometer (EDS), respectively.

3. Results and discussion

XRD patterns show that $Re_2Fe_{14}B$ is the main phase for these sintered magnets. Figure 1(a) displays the demagnetization loops for these sintered magnets, which were prepared by the dual alloy method except $(PrNd)_{15}Fe_{77}B_8$ and $(PrNd)_5Ce_{10}Fe_{77}B_8$ magnets. The variations of coercivity and energy product with the Ce atomic percent are shown in Fig. 1(b). It can be seen that a little additive amount of $(PrNd)_5Ce_{10}Fe_{77}B_8$ powders results in a dramatic drop of coercivity H_c. While, with the further increase of additive amount, the coercivity increases firstly, peaks at 6.38 kOe in $(PrNd)_{11}Ce_4Fe_{77}B_8$ magnets, and then decreases gradually. The variation of energy product (BH_{max}) follows that of coercivity with Ce content.

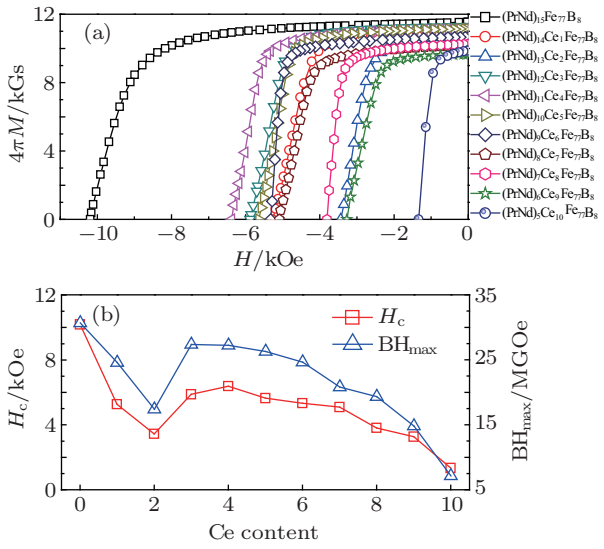


Fig. 1. (color online) (a) The demagnetization loops for the sintered magnets prepared by the dual alloy method, and (b) the variations of coercivity H_c and energy product BH_{max} with the Ce atomic percent.

Ce element substitution would result in the decrease of magnetocrystalline anisotropy and coercivity in $(NdCe)_2Fe_{14}B$ magnets,[24] but among these sintered magnets, the coercivity is abnormally dependent on the Ce content. Similar experiments on the coercivity variation were observed in Refs. [20], [25], and [26]. Coercivity is dependent not only on the intrinsic magnetic properties, but also on the microstructure. Figure 2 shows the surface micromorphology investigated by BSE for the $(PrNd)_{15}Fe_{77}B_8$, $(PrNd)_{11}Ce_4Fe_{77}B_8$, $(PrNd)_9Ce_6Fe_{77}B_8$, and $(PrNd)_5Ce_{10}Fe_{77}B_8$ magnets, respectively. For the $(PrNd)_{15}Fe_{77}B_8$ and $(PrNd)_{11}Ce_4Fe_{77}B_8$, there are some darker pores on the surface, but less amount of pores present in the $(PrNd)_9Ce_6Fe_{77}B_8$ and $(PrNd)_5Ce_{10}Fe_{77}B_8$ magnets. Possibly, the Ce element lowers the melting point of the intergranular phase and improves the wetting characteristics of the liquid phase in the sinter process,[27,28] enhancing the interfacial bond strength at the grain boundary. It can be seen that in $(PrNd)_9Ce_6Fe_{77}B_8$ and $(PrNd)_5Ce_{10}Fe_{77}B_8$ magnets there exist two regions in the intergranular phase. As shown by the arrows in Fig. 2(c), one is gray black and the other is a little brighter enveloping the gray region. Figure 3 shows the EDS intensities of Pr, Nd, Ce, and Fe for the main matrix, intergranular gray, and bright regions, respectively, in the $(PrNd)_9Ce_6Fe_{77}B_8$ magnet. The intensities of Fe are strongest in the main matrix, indicating a high content of Fe, which is well consistent with the chemical composition of main phase $(PrNdCe)_2Fe_{14}B$. The intensities of rare earth elements increase in the intergranular phase, but the intensities of Pr, Nd, Ce, and Fe are different between intergranular gray and bright regions. This fact suggests that Pr, Nd, and Ce cannot be completely dissolved with each other and the chemical composition is inhomogeneous in the intergranular phase.

The nucleation of reversed domain and coercivity are related to the intergranular rare earth-rich phase and grain boundary.[29,30] In order to explore the relationship between the coercivity and the intergranular phase, the element distribution was investigated near the grain boundary by line scanning using EDS. The intergranular phase of $(PrNd)_{15}Fe_{77}B_8$ magnets is rich in Pr and Nd elements (shown in Fig. 4(a)). As shown in Fig. 4(b), even for the addition of a little amount of $(PrNd)_5Ce_{10}Fe_{77}B_8$ powders, the Ce element is evident in the intergranular phase in the $(PrNd)_{13}Ce_2Fe_{77}B_8$ magnet. It is noted that the element segregation and phase separation were observed near the grain boundary in the $(PrNd)_{11}Ce_4Fe_{77}B_8$ magnet, in which the intergranular phase is rich in Ce but poor in Pr and Nd (shown in Fig. 4(c)). For further increase of the additive amount, the contents of Pr and Nd increase in the intergranular phase, and all of the Pr, Nd and Ce contents are high in the intergranular phase of the $(PrNd)_7Ce_8Fe_{77}B_8$ magnet (shown in Fig. 4(d)).

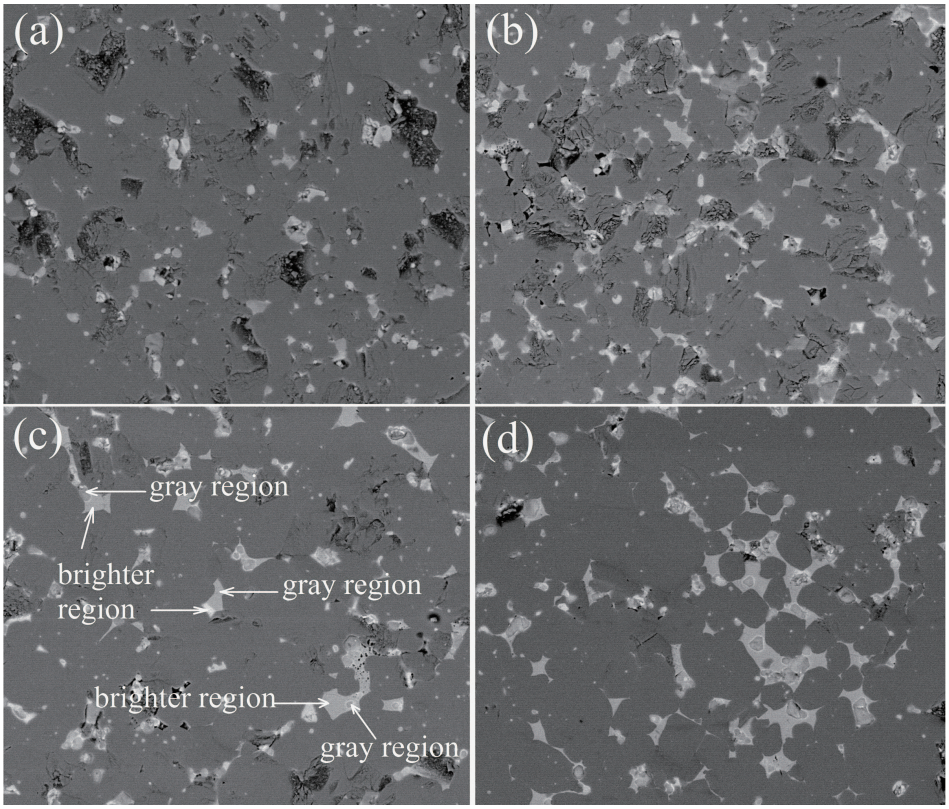


Fig. 2. (color online) The surface micromorphology investigated by BSE for the $(PrNd)_{15}Fe_{77}B_8$ (a), $(PrNd)_{11}Ce_4Fe_{77}B_8$ (b), $(PrNd)_9Ce_6Fe_{77}B_8$ (c), and $(PrNd)_5Ce_{10}Fe_{77}B_8$ (d), respectively.

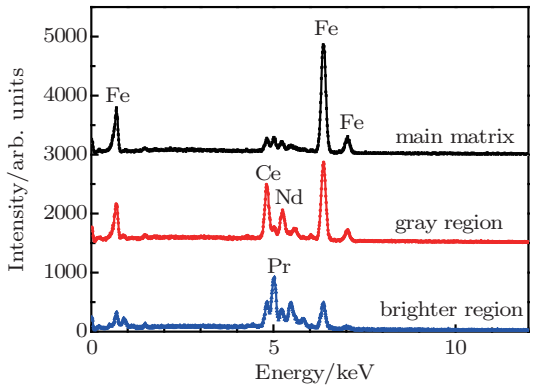


Fig. 3. (color online) The EDS intensities of Pr, Nd, Ce, and Fe for the $(PrNd)_9Ce_5Fe_{77}B_8$ magnet in the main matrix, intergranular gray, and brighter regions, respectively.

In the $(Nd_{1-x}Ce_x)_2Fe_{14}B$ ($x \leq 0.3$) magnets, Ce is predicted to have limited alloying with a preference for larger $R(4g)$ sites due to the atomic size effect, resulting in weak partial ordering.[31] This is consistent with Ce segregation near the grain boundary in this experiment for $(PrNd)_{15-x}Ce_xFe_{79}B_6$ ($x \leq 4$). The high c-axis manetocrystalline anisotropy originates from the $R(4g)$ site in the $Nd_2Fe_{14}B$ lattice.[32] Ce element aggregation in the intergranular phase and the substitution for $R(4g)$ sites may heavily ruin the magnetocrystalline anisotropy at the grain boundary and decrease the nucleation field,[33] which is likely to result in the dramatic drop of coercivity in $(PrNd)_{14}Ce_1Fe_{77}B$ and $(PrNd)_{13}Ce_2Fe_{77}B_8$ magnets. The further increase of Ce content leads to an increase of coercivity in the $(PrNd)_{12}Ce_3Fe_{77}B_8$ and $(PrNd)_{11}Ce_4Fe_{77}B_8$ magnets, but the underlying mechanism remains unclear. Similar results were reported in $(Re_{1-x}Ce_x)_2(FeCo)_{14}B$ magnets as x is in the range of 0.20–0.30,[20,25,26] and it proposed that the anomaly was possibly related to the phase separation.[25] Magnetization reversal and coercivity are strongly dependent on the self-interaction between perfect and defect regions at the grain outer layer.[34] As shown in Fig. 4(c), Ce enrichment whereas a lack of PrNd in the intergranular phase implies the inhomogeneous distribution of rare earth elements near the grain boundary, which possibly leads to an abrupt change in anisotropy and may vary the characteristics of self-interaction at the grain outer layer. Further research is being planned to investigate the abnormal dependence of coercivity on Ce content by checking the phase separation near the grain boundary and the variation in anisotropy. For further increase of the $(PrNd)_5Ce_{10}Fe_{77}B_8$ additive amount, the Ce content increases in the magnets, and the homogeneity of chemical composition near the grain boundary is improved, but the coercivity decreases gradually.

For comparasion, the $(PrNdCe)_2Fe_{14}B$ magnets were prepared by the conventional powder metallurgy method using the same sintering and annealing process. Figure 5 shows the demagnetization loops for two types of magnets with the same nominal compositions of the $(PrNd)_9Ce_6Fe_{77}B_8$, $(PrNd)_8Ce_7Fe_{77}B_8$, and $(PrNd)_7Ce_8Fe_{77}B_8$ magnets, re-

spectively. The suffix (S) denotes the magnets prepared by the conventional method. It can be seen that the coercivity of the magnets prepared by the dual alloy method is higher than that of corresponding conventional magnets. In addition, compared with that in $(PrNd)_5Ce_{10}Fe_{77}B_8$, the coecivity improves largely in $(PrNd)_7Ce_8Fe_{77}B_8$ and $(PrNd)_8Ce_7Fe_{77}B_8$ magnets (shown in Fig. 1). These facts indicate the advantage of the dual alloy approach for improving the magnetic properties in Ce-rich $(PrNdCe)_2Fe_{14}B$ magnets.[35] It is noted that the remanence of the sintered magnets is low due to the high rare earth content. Properly reducing the rare earth amount in (PrNdCe)–Fe–B could improve saturation magnetization, and doping Cu, Al, and/or Zn is a feasible way to enhance the coercivity, so it has much room to improve the energy product in this type of magnets prepared by the dual alloy method.

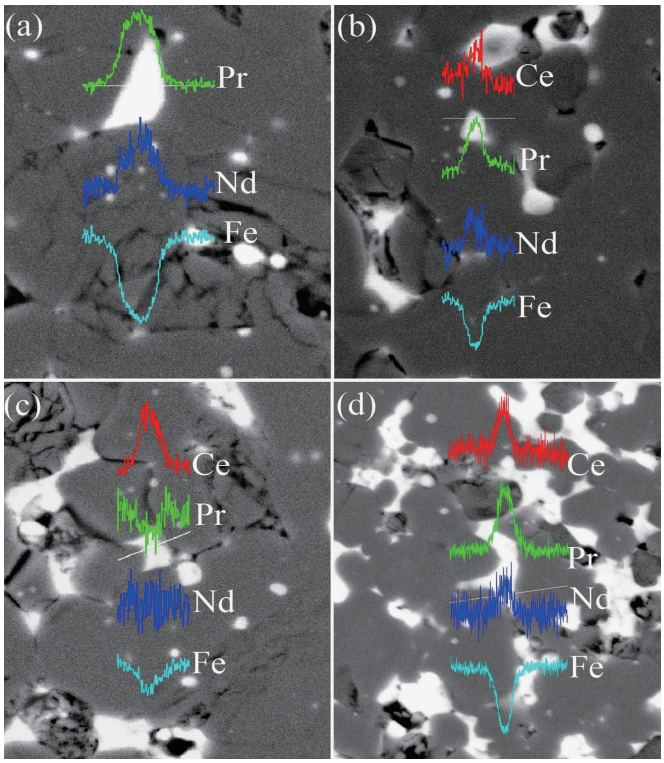


Fig. 4. (color online) The element distribution near the grain boundary for $(PrNd)_{15}Fe_{77}B_8$ (a), $(PrNd)_{13}Ce_2Fe_{77}B_8$ (b), $(PrNd)_{11}Ce_4Fe_{77}B_8$ (c), and $(PrNd)_7Ce_8Fe_{77}B_8$ (d) magnets, respectively.

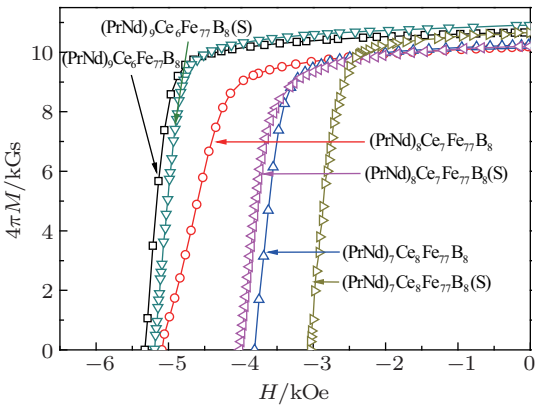


Fig. 5. (color online) The demagnetization loops for the two types of magnets with nominal compositions, $(PrNd)_9Ce_6Fe_{77}B_8$, $(PrNd)_8Ce_7Fe_{77}B_8$, and $(PrNd)_7Ce_8Fe_{77}B_8$, and the suffix (S) denotes the magnets prepared by the conventional method.

4. Conclusions

In summary, $(PrNdCe)_{15}Fe_{77}B_8$ sintered magnets were prepared using the dual alloy method by mixing $(PrNd)_5Ce_{10}Fe_{77}B_8$ with $(PrNd)_{15}Fe_{77}B_8$ powders. The magnetic properties is abnormally dependent on the Ce atomic percent, and the corecivity peak at 6.38 kOe in $(PrNd)_{11}Ce_4Fe_{77}B_8$ magnets. In Ce-rich magnets prepared by the dual alloy method, coercivity is higher than that of corresponding magnets prepared by the conventional method. It is expected that these investigations could serve as a reference for optimizing the composition design in preparing high abundant rare earth magnets.

References

[1] Sagawa M, Fujimura S, Togawa N, Yamamoto H and Matsuura Y 1984 *J. Appl. Phys.* **55** 2083
[2] Croat J J, Herbst J F, Lee R W and Pinkerton F E 1984 *Appl. Phys. Lett.* **44** 148
[3] Cai L W, Guo S, Ding G F, Chen R J, Liu J, Lee D and Yan A R 2015 *Chin. Phys. B* **24** 097505
[4] Herbst J F 1991 *Rev. Mod. Phys.* **63** 819
[5] Burzo E 1998 *Rep. Prog. Phys.* **61** 1099
[6] Wang X C, Zhu M G, Li W, Zheng L Y, Zhao D L, Du X and Du A 2015 *Electron. Mater. Lett.* **11** 109
[7] Coey J M D 2012 *Scripta Mater.* **67** 524
[8] Chang H W, Chen C H, Hsieh C C and Chang W C 2011 *J. Nanosci. Nanotechnol.* **11** 2756
[9] Zhang M, Li Z B, Shen B G, Hu F X and Sun J R 2015 *J. Alloys Compd.* **651** 144
[10] Skoug E J, Meyer M S, Pinkerton F E, Tessema M M, Haddad D and Herbst J F 2013 *J. Alloys Compd.* **574** 552
[11] Zhang X F, Shi Y, Ma Q, Liu Y L, Shi M F, Li Y F, Wang G F and Zhao Z R 2015 *Rare Metal. Mat. Eng.* **44** 748
[12] Abache C and Oesterreicher J 1986 *J. Appl. Phys.* **60** 3671
[13] Capehart T W, Mishra R K, Meisner G P, Fuerst C D and Herbst J F 1993 *Appl. Phys. Lett.* **63** 3642
[14] Yan C J, Guo S, Chen R J, Lee D and Yan A R 2014 *Chin. Phys. B* **23** 107501
[15] Herbst J F, Meyer M S and Pinkerton F E 2012 *J. Appl. Phys.* **111** 07A718
[16] Zhou S X, Wang Y G and Høier R 1994 *J. Appl. Phys.* **75** 6268
[17] Xing M Y, Han J Z, Lin Z, Wan F W, Lin C, Liu S Q, Wang C S, Yang J B and Yang Y C 2012 *J. Magn. Magn. Mater.* **331** 140
[18] Li D and Bogatin Y 1991 *J. Appl. Phys.* **69** 5515
[19] Zhou Q Y, Liu Z, Guo S, Yan A R and Lee D 2015 *IEEE Trans. Magn.* **51** 2104304
[20] Yan C J, Guo S, Chen R J, Lee D and Yan A R 2014 *IEEE Trans. Magn.* **50** 2102605
[21] Li W, Li A, Feng H, Huang S, Wang J and Zhu M 2015 *IEEE Trans. Magn.* **51** 2103603
[22] Yan C, Guo S, Chen R, Lee D and Yan A 2014 *IEEE Trans. Magn.* **50** 2104604
[23] Zhu M G, Li W, Wang J D, Zheng L Y, Li Y F, Zhang K, Feng H B and Liu T 2014 *IEEE Trans. Magn.* **50** 1000104
[24] Li Z B, Shen B G, Zhang M, Hu F X and Sun J R 2015 *J. Alloys Compd.* **628** 325
[25] Pathak A K, Khan M, Gschneidner Jr K A, McCallum R W, Zhou L, Sun K, Dennis K W, Zhou C, Pinkerton F E, Kramer M J and Pecharsky V K 2015 *Adv. Mater.* **27** 2263

[26] Pei K, Zhang X, Lin M and Yan A 2016 *J. Magn. Magn. Mater.* **398** 96

[27] Huang S L, Feng H B, Zhu M G, Li A H, Li Y F, Sun Y C, Zhang Y and Li W 2015 *Int. J. Miner. Metall. Mater.* **22** 417

[28] Huang S L, Feng H B, Zhu M G, Li A H, Zhang Y and Li W 2014 *Aip Adv.* **4** 107127

[29] Kronmüller H, Durst K D and Sagawa M 1988 *J. Magn. Magn. Mater.* **74** 291

[30] Ju J Y, Tang X, Chen R J, Wang J Z, Yin W Z, Lee D and Yan A R 2015 *Chin. Phys. B* **24** 017504

[31] Alam A, Khan M, Mccallum R W and Johnson D D 2013 *Appl. Phys. Lett.* **102** 042402

[32] Haskel D, Lang J C, Islam Z, Cady A, Srajer G, Veenendaal M V and Canfield P C 2005 *Phys. Rev. Lett.* **95** 217207

[33] Chu L H, Liu Y, Li J, Ma Y L and Li C Y 2012 *IEEE Trans. Magn.* **48** 2092

[34] Li Z B, Shen B G, Zhang M, Zhang Y, Hu F X and Sun J R 2015 *Appl. Phys. Lett.* **106** 042403

[35] Zhu M G, Han R, Li W, Huang S L, Zheng D W, Song L W and Shi X N 2015 *IEEE Trans. Magn.* **51** 2104604